

AD-775 639

CONDUCTION MECHANISMS IN THICK FILM  
MICROCIRCUITS

R. W. Vest

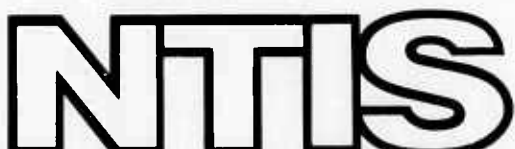
Purdue Research Foundation

Prepared for:

Defense Advanced Research Projects Agency

1 February 1974

DISTRIBUTED BY:



National Technical Information Service  
U. S. DEPARTMENT OF COMMERCE  
5285 Port Royal Road, Springfield Va. 22151

AD775639

Semi-Annual Technical Report  
for the Period 7/1/73-12/31/73

Conduction Mechanisms in Thick Film Microcircuits

Grant Number: DAHC15-73-G8

ARPA Order No.: 1001/192

Grantee: Purdue Research Foundation

Principal Investigator: R. W. Vest  
(317) 749-2601

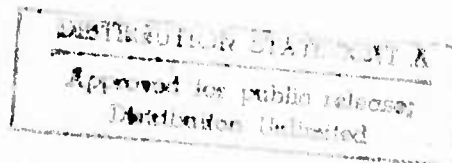
Effective Date of Grant: 7/1/73

Grant Expiration Date: 6/30/74

Amount of Grant: \$77,923

February 1, 1974

Reproduced by  
NATIONAL TECHNICAL  
INFORMATION SERVICE  
U S Department of Commerce  
Springfield VA 22151



## Forward

Research described in this report constitutes the seventh six months effort under two grants from the Defense Advance Research Projects Agency, Department of Defense, under the technical cognizance of Dr. Norman Tallan, Aerospace Research Laboratories, U. S. Air Force. The research was conducted in the Turner Laboratory for Electroceramics, School of Electrical Engineering and School of Materials Engineering, Purdue University, West Lafayette, Indiana 47907, under the direction of Professor R. W. Vest. Contributing to the project were Assistant Professor G. L. Fuller, Mr. M. S. Allison, Mr. D. J. Deputy, Mr. E. M. Miller, Mr. M. Myint, Mr. A. N. Prabhu, Mr. R. L. Reed, and Mr. J. L. Wright.

## ABSTRACT

The viscosity and surface tension of 63% PbO-25% B<sub>2</sub>O<sub>3</sub>-12% SiO<sub>2</sub> glass were measured from 650° to 800°C. The initial stage sintering kinetics were directly measured by observing the rate of neck growth between adjacent glass spheres in the temperature range 480° to 550°C. The sintering kinetics agree with a Newtonian viscous flow mechanism and further, show good agreement with the extrapolation of the viscosity and surface tension data.

Studies of the electrical properties of a single contact between small RuO<sub>2</sub> single crystals gave insight into a charge transport mechanism not involving well sintered contacts. Electrical continuity quickly developed between crystals placed in contact after having been previously coated with glass. The glass not only does not impede charge transport, but enhances the rate of formation of an electrically quiet, low resistance contact. Studies of test resistors made with RuO<sub>2</sub> particles one thousand times greater in diameter than normal for a thick film resistor confirmed the general observations in the single contact studies, namely, that a low resistivity contact with a TCR below that of RuO<sub>2</sub> can be developed without true sintering between RuO<sub>2</sub> particles.

Studies of evaporation and decomposition of a new screening agent system involving polyalphamethylstyrene are presented. This system seems promising in that complete organic removal is obtained at a lower temperature than with the ethyl cellulose-butyl carbitol system previously employed.

## TABLE OF CONTENTS

	Page
I. Introduction	1
II. Microstructure Development	3
A. Glass Viscosity	3
B. Glass Surface Tension	7
C. Glass Sintering	8
III. Resistor Firing	14
A. Crossed Crystal	14
B. Large Particle Resistors	22
C. Low Temperatures Measurements	27
IV. Industrial Coupling	31
A. Search for New Screening Agent	31
B. Evaluation for Polystyrene	32
V. Summary and Future Plans	39
A. Microstructure Development	39
B. Charge Transport Mechanisms	39
C. Test of Models	40
VI. References	41
VII. Distribution List	43

List of Figures

<u>Figure</u>		<u>Page</u>
1	Viscosity Apparatus	4
2	Temperature Dependence of Viscosity of Lead Borosilicate Glass	6
3	Surface Tension of Lead Silicate and Lead Borosilicate Glasses	9
4	Initial Stage Sintering Kinetics for Glass Spheres	11
5	Temperature Dependence of Glass Viscosity	13
6	Photomicrograph of Massive Crystals with Single Point Contact	16
7	Resistance versus Temperature of Crossed Crystals	18
8	Photomicrographs of Small Crossed Single Crystals	20
9	Resistance and TCR of Small Crossed Crystals	21
10	Large Particle Resistors	24
11	Resistance versus Temperature of Large Particle Resistors	25
12	Resistance versus Temperature During Firing of Large Particle Resistors	26
13	Low Temperature Resistance and Temperature Measuring Fixture	28
14	Normalized Resistance of Resistors versus Low Temperature	30
15	Evaporation of Polyalphaethylstyrene at Constant Temperatures	34
16	Comparison of Evaporation Rates	35

List of Figures (continued)

<u>Figure</u>		<u>Page</u>
17	Effect of Screening Agent Residues	36
18	Comparison of Viscosity versus Shear Rate	38

## 1. Introduction

Advances in thick film technology have been hindered by an inadequate understanding of the relationships between the physical properties of the ingredient materials and the electrical properties of the resulting resistors and conductors. The lack of a predictive model of the conduction mechanism has hampered the development of new materials, as well as the improvement of existing systems. The two primary concerns of the present research program in the area of resistor technology are the development of adequate models to describe the "Blending Curve Anomaly" and the "TCR Anomaly." The "Blending Curve Anomaly" refers to the often reported observation that with oxidic conductors and glass the sheet resistance varies monotonically from very low (e.g., 1 v/o) to very high conductive concentrations; whereas, with noble metal conductives and glass electrical continuity is not achieved until the amount of conductive approaches 50 v/o. The primary scientific question is: what are the driving forces which are responsible for the formation of continuous conducting paths along the length of the resistor at such low concentrations of the conductive? The "TCR Anomaly" refers to the fact the temperature coefficient of resistance of a resistor is much lower than the TCR of any of the individual ingredients from which it was made. The primary scientific question is: what is the mechanism by which electric charge is transported?

The primary thrust of the experimental program is to relate electrical properties of the thick films to the materials properties and processing conditions through microstructure. The materials properties to be correlated

are: resistivity, temperature coefficient of resistivity, coefficient of thermal expansion, interfacial energy, particle shape, size and size distribution, and chemical reactivity with other constituents. The processing conditions to be correlated are time, temperature and atmosphere during firing. The specific objectives of the program are:

1. Determine the dominant sintering mechanisms responsible for microstructure development and establish the relative importance of the various properties of the ingredient materials.
2. Determine the dominant mechanisms limiting electrical charge transport, and establish the relative importance of the various properties of the ingredient materials.
3. Develop phenomenological models to interrelate the various materials properties with systems performance.

Earlier work in these three areas have been previously reported {1-6}.

## II. Microstructure Development

The electrical properties of a thick film resistor depend directly on the microstructure that is formed during the firing cycle, normally executed with a tunnel kiln. The proposed model of microstructural development {7} predicts a sequence of steps that begins with the sintering of the glass; it has been determined that this is the initial step. In order to quantify the model and thereby improve its usefulness in mass production environments three types of measurements have been performed. The viscosity and surface tension of the glass have been directly measured as functions of temperature; these are the two most critical parameters which control the kinetics of viscous flow sintering. In addition, neck growth measurements during the initial stages of glass sintering have been conducted with the hot stage video-metallograph described earlier {8}. The results of the three measurements are consistent with one another.

### A. Glass Viscosity

The viscosity of the molten glass was measured by the sphere method {9}. A gold ball, 0.86 cm in diameter was suspended by a thin platinum wire from the sample pan of an automatic recording Ainsworth microbalance as shown in Fig. 1. The balance has an accuracy and resolution capability of about 5 $\mu$ g and an automatic range of 100 mg. All small weight changes are normally detected by a linear variable differential transformer whose output is proportional to the beam displacement, and this signal is recorded on a strip chart. Therefore, the chart recorder can be calibrated to directly measure the displacement of the ball in the glass as a function of time. For the balance utilized in this study, full scale on the chart recorder (10 inches) corresponded to 0.041 inches travel of the ball.

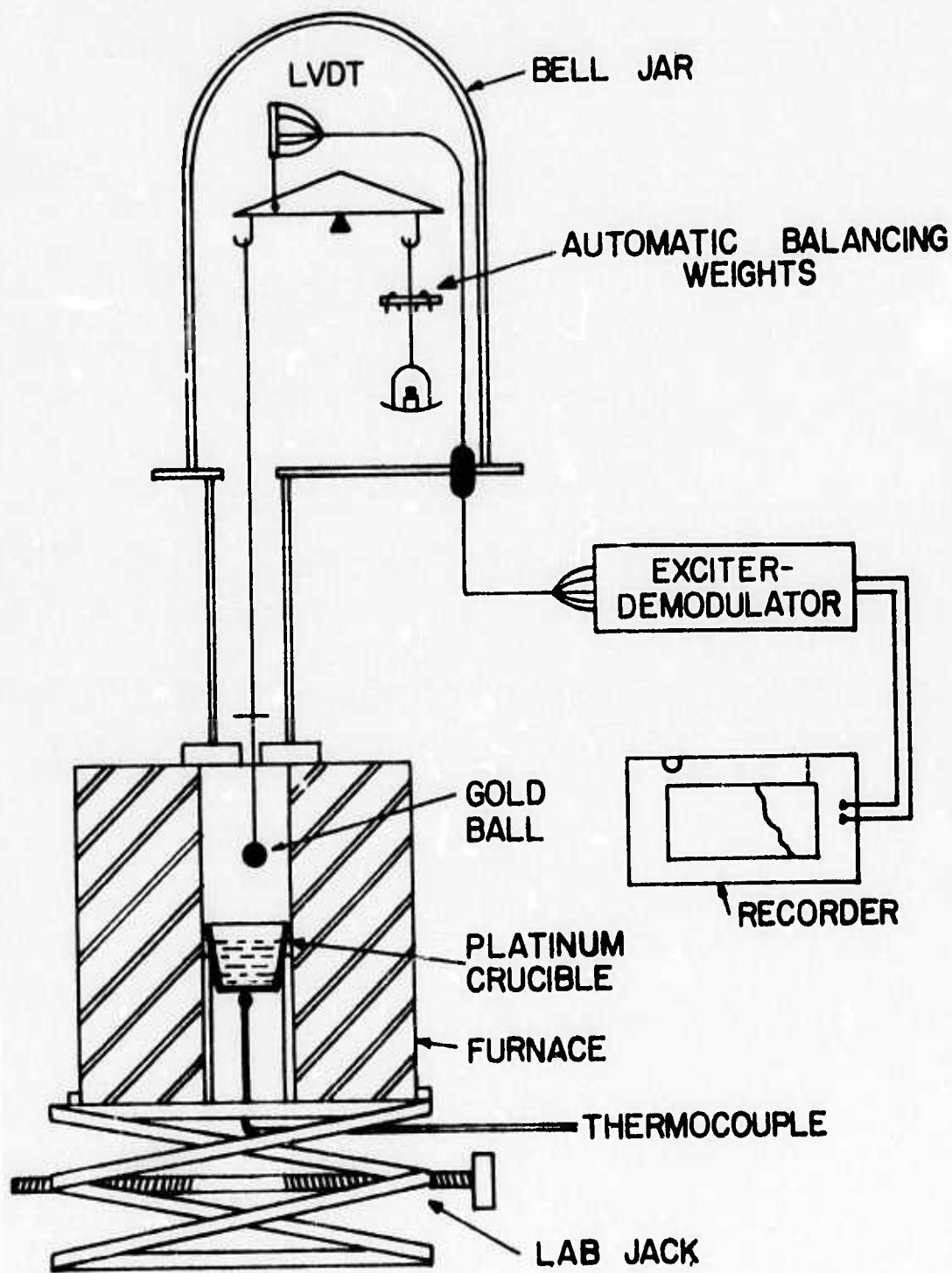


FIGURE 1 -- VISCOSITY APPARATUS

A platinum crucible  $1\frac{1}{2}$ " deep was filled with glass and placed on a ceramic support so that it was centered in a vertical cylindrical furnace that could be raised or lowered by a lab jack. The temperature of the glass was measured by a chromel-alumel thermocouple placed in contact with the bottom of the crucible. The upward and downward motion of the ball in the molten glass was recorded after adding weights to or removing weights from the tare pan. Force versus velocity data are plotted for both the upward and downward motion. These plots are straight lines and the mean of the two slopes is used for the direct calculation of the viscosity using the formula

$$\eta = \frac{s g . Fa}{3\pi d} , \text{ in which}$$

s = mean slope of the force versus velocity plot. gm/cm/sec

g = gravitational constant = 980 dynes/sec

Fa = Faxen correction factor

$$= 1 - 2.104 \frac{d}{D} + 2.09 \left(\frac{d}{D}\right)^3 - 0.95 \left(\frac{d}{D}\right)^5$$

d = diameter of the sphere

D = diameter of the crucible

In order to check the accuracy of the experimental method, the viscosity of a Brookfield viscosity standard\* (Fluid 100,000) was measured and compared with the reported value of 953.5 poise. The measured value, 1069, is within 12.1%.

The viscosity results are shown in Fig. 2. The plot of the logarithm of viscosity versus reciprocal temperature of the lead borosilicate glass is a straight line over the temperature range studied confirming the

\*Brookfield Engineering Laboratories, Inc., 240 Cushing Street, Stoughton, Mass. 02072.

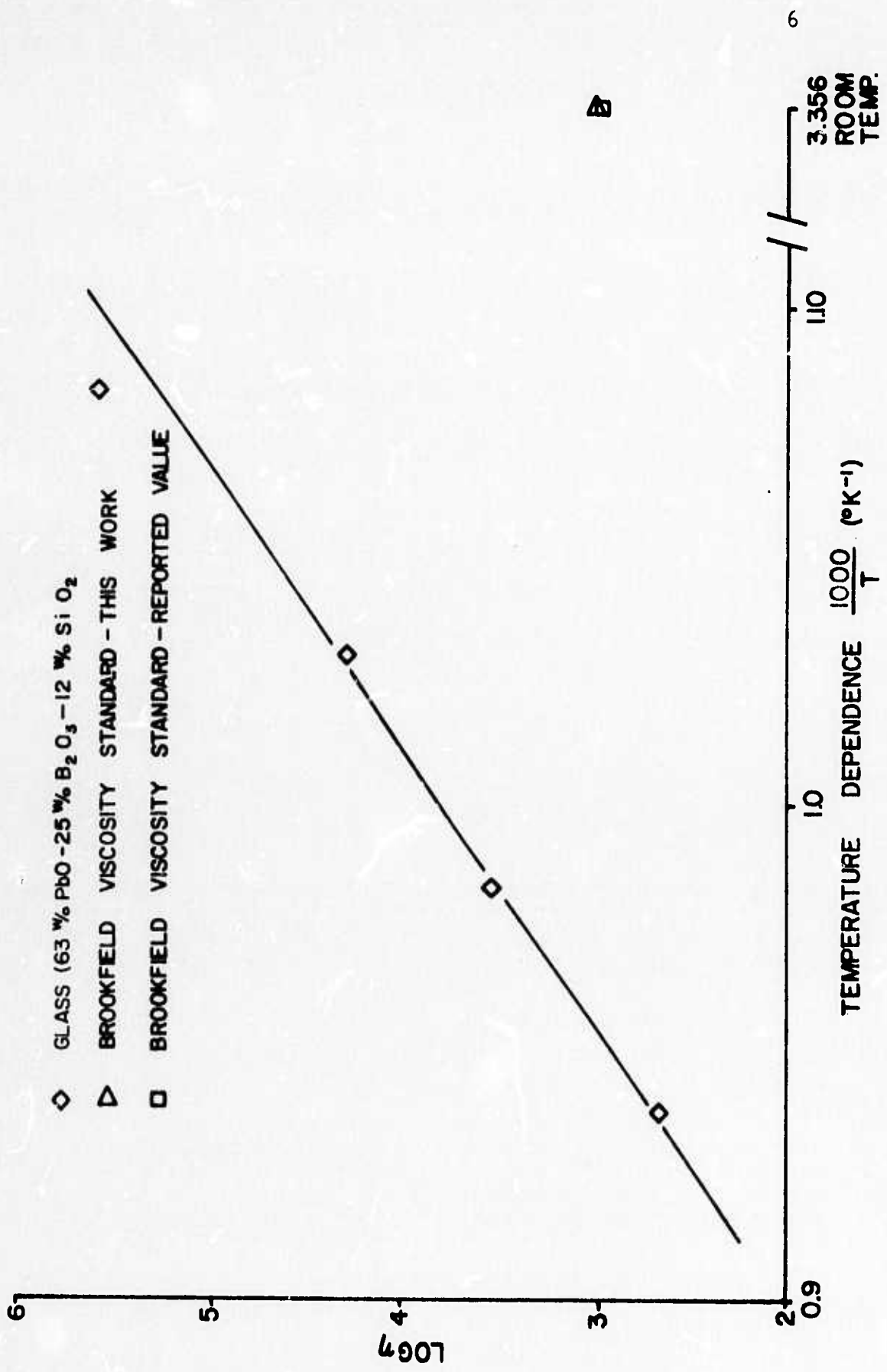


FIGURE 2 -- TEMPERATURE DEPENDENCE OF VISCOSITY OF LEAD BOROSILICATE GLASS

anticipated exponential temperature dependence of the viscosity. The viscosity is quite low near 800°C, an important factor in the micro-structure development of the thick film resistors for typical firing conditions.

#### B. Glass Surface Tension

Surface tension of the glass was measured using the modified dipping cylinder method {10} with an experimental set-up similar to that shown in Fig. 1. The gold ball used for the viscosity measurements was removed and a platinum cylinder, 0.5 inches in diameter, 0.5 inches high and 0.005 inches thick suspended by a platinum hang down wire from the sample pan of the Ainsworth balance. The crucible was raised until the bottom edge of the platinum cylinder was below the surface of the glass and the crucible was then slowly lowered. The downward force on the cylinder caused by the surface tension of the glass was recorded on a chart. After the cylinder breaks away from the glass the weight of the cylinder and any glass retained on the rim of the cylinder was subtracted from the terminal force before break-away. The terminal force,  $W_{\max}$ , was used to calculate the surface tension of the glass,  $\gamma$  with the equation

$$\gamma = \frac{gW_{\max}}{4\pi R} \left\{ 1 - \frac{2.8284\delta}{\sqrt{hR}} - \frac{0.6095\delta}{R} + \frac{3\delta^2}{hR} + \frac{2.585\delta^2}{R\sqrt{hR}} \right\} = \frac{0.371\delta^2}{R^2}$$

where  $\gamma$  = surface tension in dynes/cm

$$h = \frac{W_{\max}}{\pi R^2 \rho}$$

$W_{\max}$  = maximum pull in grams exerted on the cylinder

$\rho$  = density of the glass

R = mean radius of the cylinder

$2\delta$  = thickness of the cylinder

The densities of the glass at the temperatures of the experiments were determined by the extrapolation of the low temperature expansion data [11].

Preliminary measurements were carried out with an 85.08 w/o PbO - 14.92 w/o SiO<sub>2</sub> glass in order to verify the experimental technique by comparison with previously reported values for SiO<sub>2</sub> glasses [12]. The surface tension of the 85.08 w/o PbO - 14.92 w/o SiO<sub>2</sub> glass shown in Fig. 3 is seen to be consistent with the previously reported values of viscosity of these similar glasses. The data plotted in Fig. 3 show that the surface tension of the PbO - B<sub>2</sub>O<sub>3</sub> - SiO<sub>2</sub> glass increases with decreasing temperature, especially below 750°C. Such a negative temperature coefficient of surface tension has been previously reported for PbO-B<sub>2</sub>O<sub>3</sub> glasses having 50 - 80 w/o PbO [12]. Clearly, the kinetics of microstructural development are strongly dependent on the temperature over the range 650°C to 800°C.

### C. Glass Sintering

The apparatus to study the neck growth between adjacent spherical particles of the glass during sintering and the results of the preliminary experiments have been described in the previous reports. [13] Hence, only the experimental results on glass sintering are reported here. The neck growth between glass spheres ranging from 180-250 um. in diameter was measured as a function of time at five different temperatures from 480°C-550°C. In each case the neck growth data, including time and temperature were recorded continuously on video tape during the complete sintering process.

Assuming that Newtonian viscous flow is the predominant mechanism for the sintering of glass, the relationship between neck radius and time t

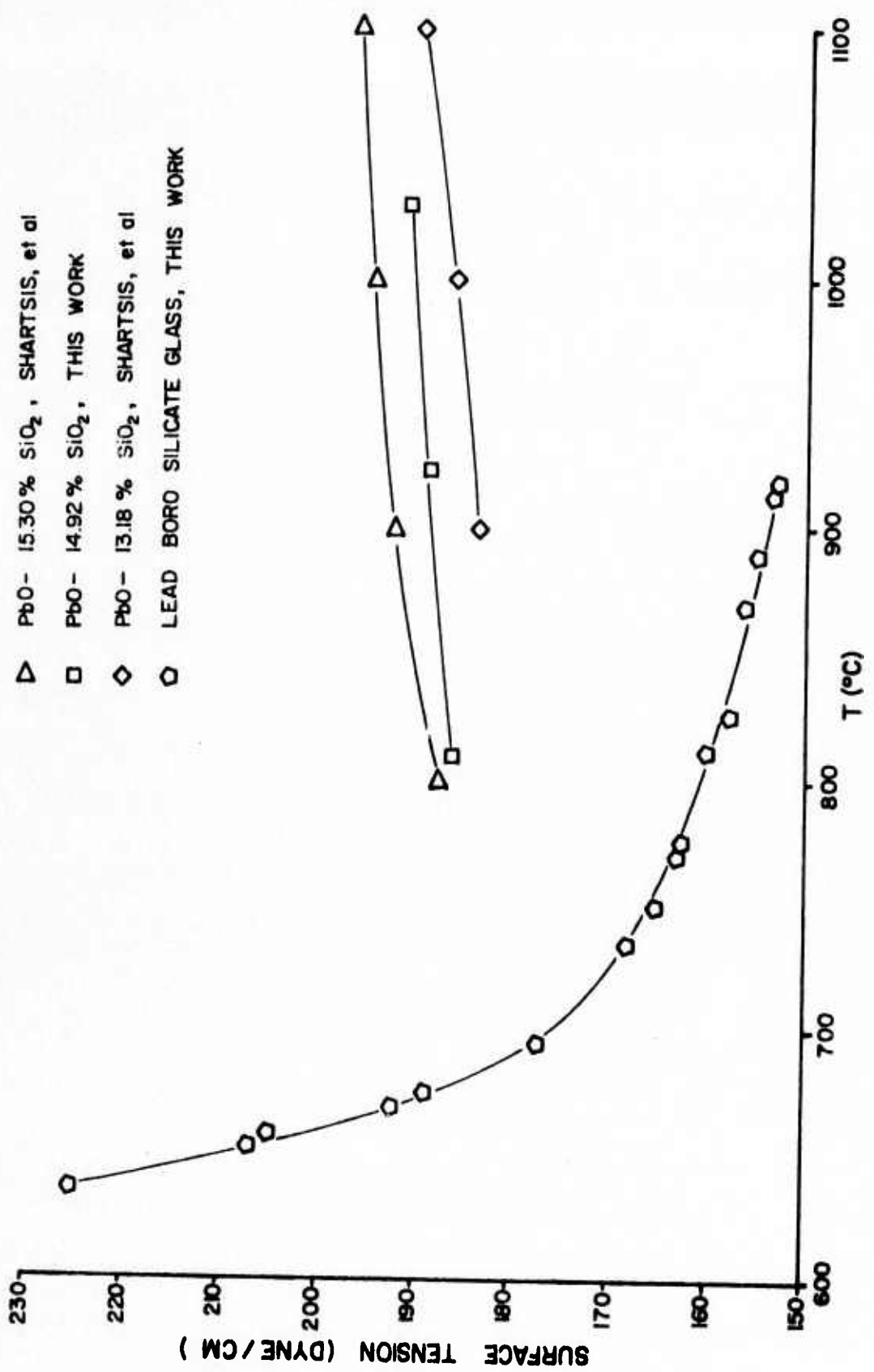


FIGURE 3 -- SURFACE TENSION OF LEAD SILICATE AND LEAD BOROSILICATE GLASSES

at any particular temperature can be written as:

$$\left(\frac{\Delta}{a}\right)^2 = \frac{3}{2} \frac{\gamma t}{a\eta} \quad (1)$$

where  $a$  is the radius of the glass spheres before sintering, and  $\gamma$  and  $\eta$  are respectively surface tension and viscosity of the glass at that temperature. Therefore, a plot of  $\left(\frac{\Delta}{a}\right)^2$  versus  $t$  should be a straight line. The predicted behavior was observed at all five temperatures as can be seen in Figs. 4a and 4b. It can, therefore, be concluded that Newtonian viscous flow is the predominant mechanism for the sintering of the lead borosilicate glass.

Viscosity values computed from the slopes of the  $\left(\frac{\Delta}{a}\right)^2$  versus  $t$  plots are plotted in Fig. 4 along with the values extrapolated from Fig. 2. The surface tension values at the experimental temperatures required for computation of the viscosity were obtained by extrapolation of the data shown in Fig. 3. The magnitudes of the viscosity values obtained by the two methods are in good agreement considering the uncertainties in the extrapolation of the viscosity and surface tension plots, but the temperature dependence of the viscosity calculated from the sintering data is greater than that shown by the extrapolated data. The viscosity measurements by the sphere method were carried out at temperatures much greater than the softening point of the glass ( $480^{\circ}\text{C}$ ), whereas the sintering data were obtained at temperatures near the softening point. The differences in the slopes could well be due to actual differences in the activation energies in the different temperature ranges.

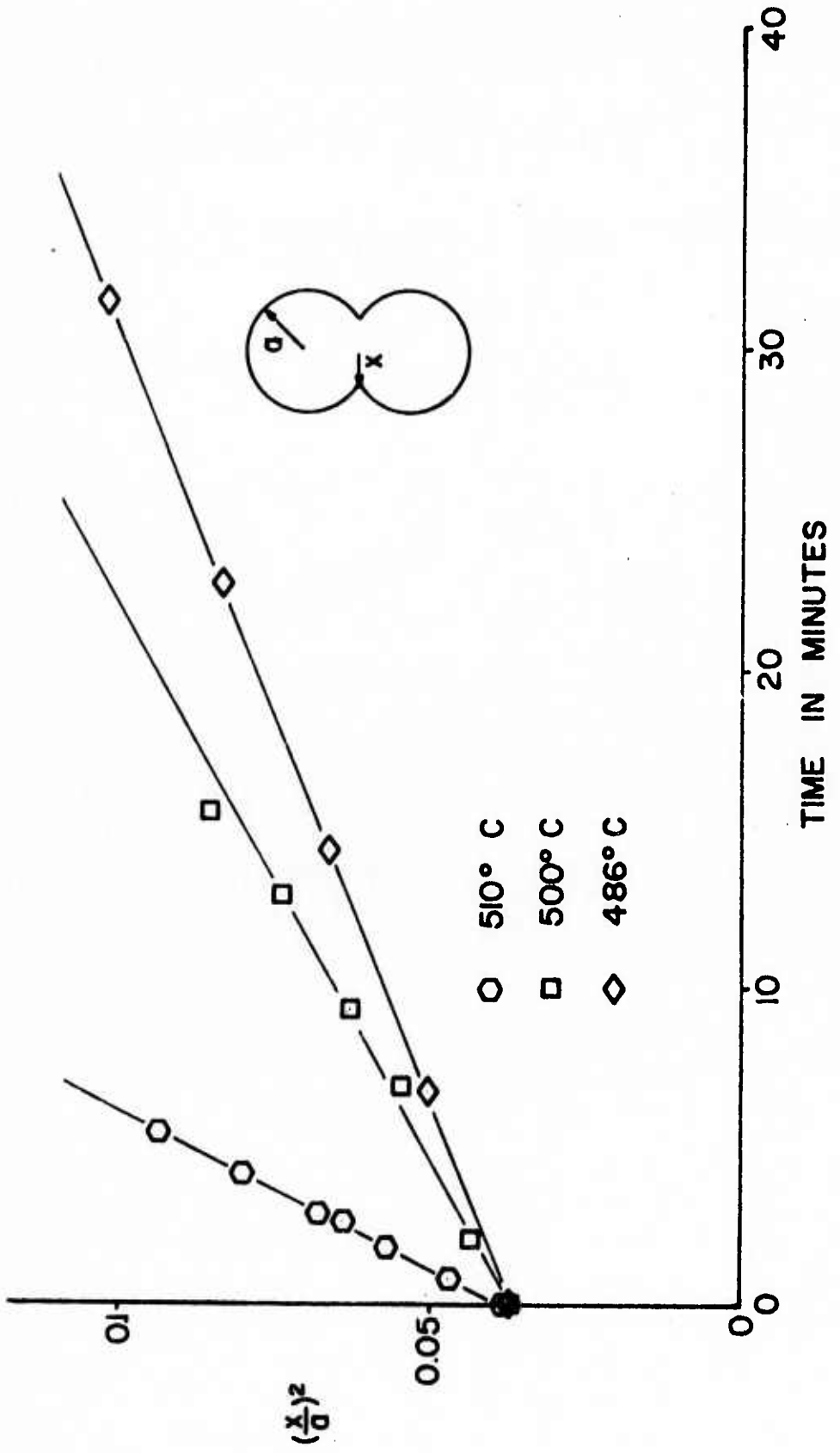


FIGURE 4A-- INITIAL STAGE SINTERING KINETICS FOR GLASS SPHERES

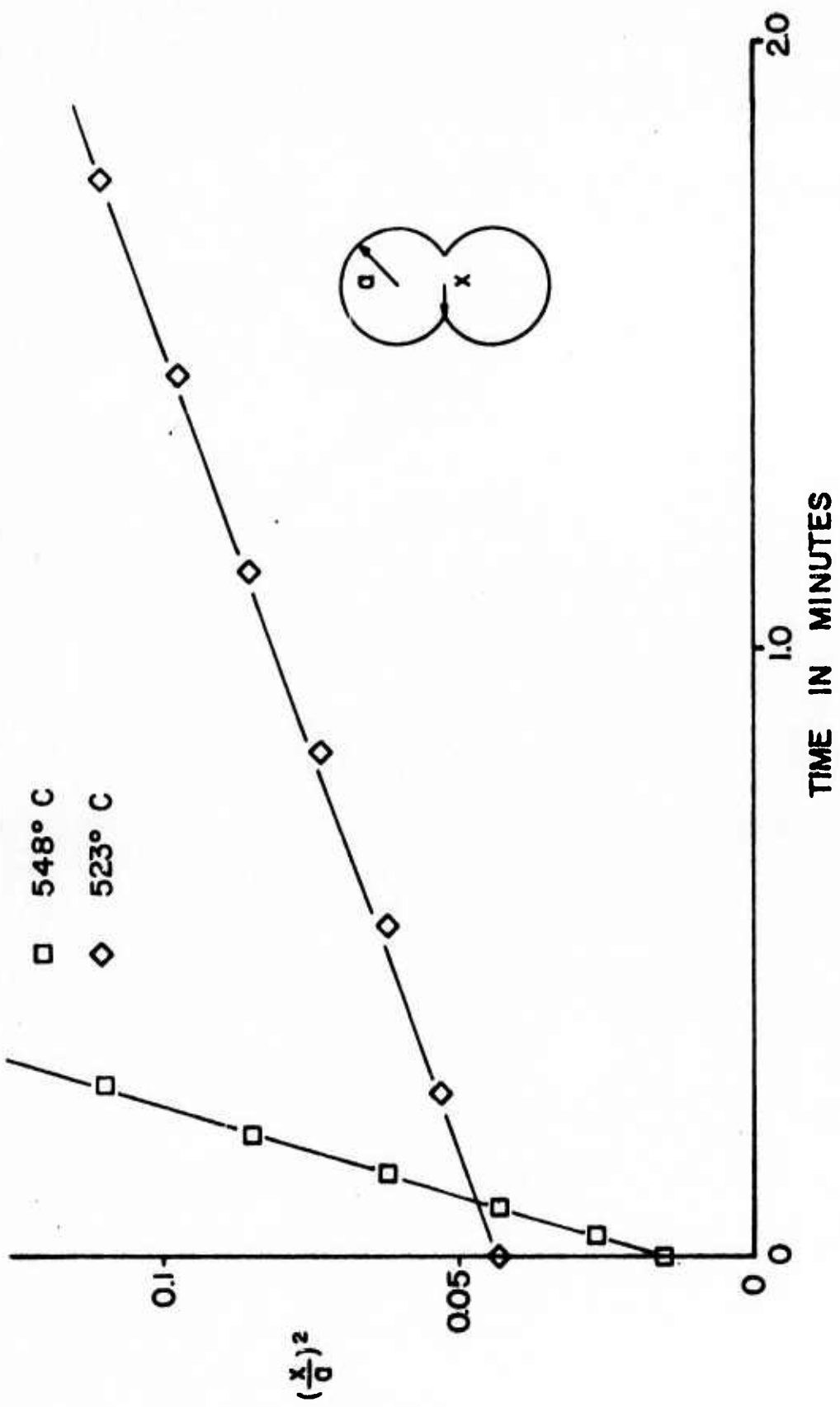


FIGURE 4B -- INITIAL STAGE SINTERING KINETICS FOR GLASS SPHERES

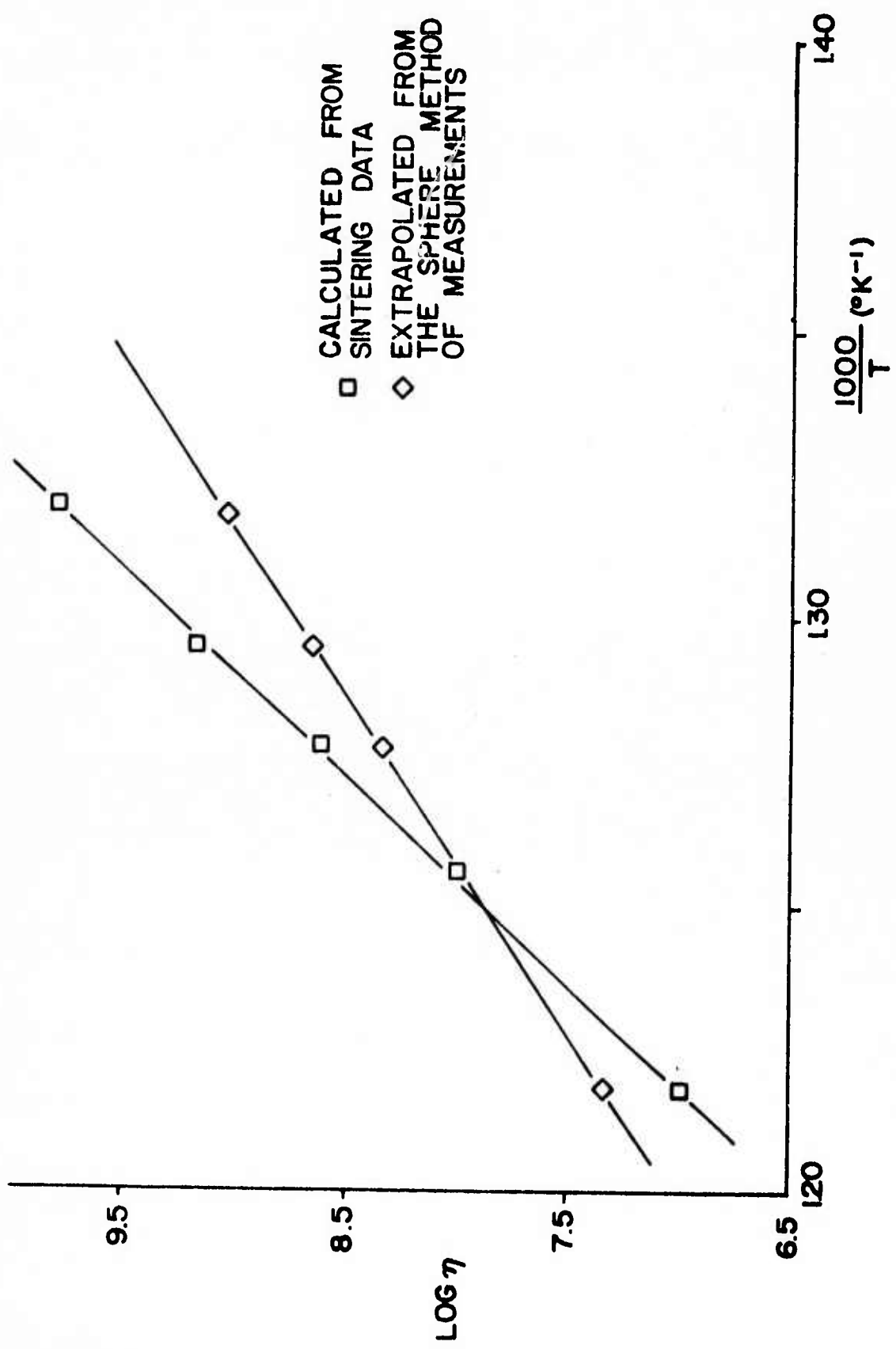


FIGURE 5 -- TEMPERATURE DEPENDENCE OF GLASS VISCOSITY

### III. Resistor Firing

#### A. Crossed Crystals

Single massive crystals of RuO<sub>2</sub> have a temperature coefficient of resistance (TCR) at room temperature of about +5000 ppm. The TCR of typical RuO<sub>2</sub> powder used in resistors is not known but is probably at least +1500 ppm. {14} Since resistors routinely have TCR's that are <+500 ppm, and sometimes negative, it is likely that the low TCR is due to the electrical properties of the "contact" between adjacent particles. Since adjacent particles of powder in a glass matrix are too small to work with, experiments involving two contacting massive single crystals have been continued in order to determine the electrical properties of this interface region with the hope of obtaining results that could be correlated to resistor properties.

Results obtained with the first such sample were reported earlier {15}. Two single crystals were mounted with a single point of contact and leads suitable for four terminal resistance measurements were attached. Glass powder was placed at the point of contact and the sample was then repeatedly heated to high temperatures and cooled to determine resistance versus temperature. The resistance of the sample was 10-20 ohms and erratic during initial heating but decreased and stabilized at temperatures beyond the softening point of the glass. The TCR during subsequent firings remained less than that of the single crystals, about 2400 ppm/<sup>o</sup>C, and the resistance versus temperature graph had a "bump" that is common with many resistor samples. Although it was believed that glass diffused into the contact areas, there was no direct evidence that this had occurred.

The slow firing of resistors discussed in the previous report [16] showed sequential stages of development with more negative TCR's near the beginning. In an attempt to explore this phenomenon further additional samples of crossed crystals precoated with glass were prepared in order measure resistance values very early in contact formation. To accomplish this, a single crystal of  $\text{RuO}_2$ , approximately  $80\mu\text{m}$  in diameter by 2 mm long, was mounted on two 5 mil platinum wires and held in place with Englehard 6082 platinum paste and 1 mil platinum wires wrapped around both the crystal and the 5 mil lead wires. Glass powder was then applied and heated to form a thin insulating film over the surface of the crystal. A second crystal of similar size was mounted in the same manner and then placed in contact with the first crystal. Figure 6 shows the mounted crystals after several firings with some additional glass added at the point of contact for increased strength. Two samples of this type were prepared.

The crystals were heated to about  $720^{\circ}\text{C}$  and maintained at constant temperature until the sample resistance decreased from initially infinite resistance. The decreasing resistance associated with initial contact formation was detected with a micro-switch mounted on the resistance chart recorder that detected the motion of the pen unit. At this time (after about  $1\frac{1}{2}$  days of firing time) the sample was quenched to study the behavior near room temperature by moving the sample in the push rod furnace. Although the TCR was always significantly lower than  $+5000 \text{ ppm}/^{\circ}\text{C}$ , the early quenchings resulted in erratic resistance at temperatures above room temperature. Considerable improvement in sample life was obtained by quenching to the annealing temperature of the glass ( $440^{\circ}\text{C}$ ) and holding for 8 hours.

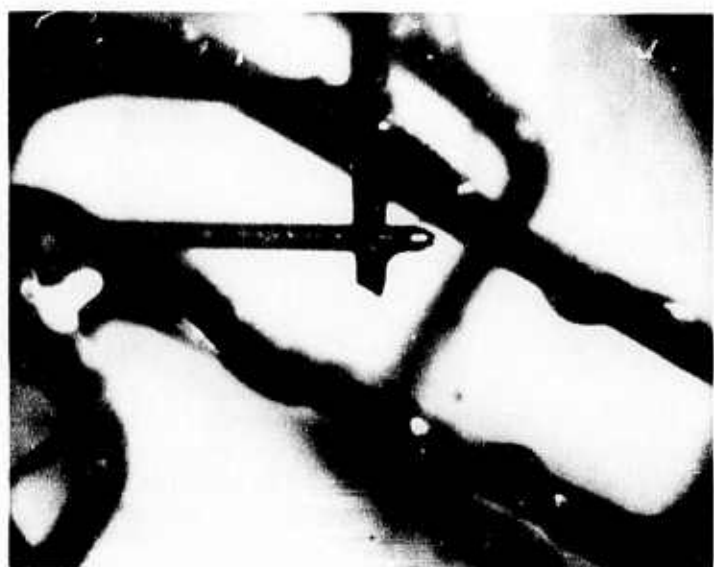


Figure 6. Photomicrograph of Massive Cyrstals with Single Point Contact. (50X)

Figure 7 shows typical behavior of both crossed crystal samples plotted as normalized resistance versus temperature after repeated firing cycles. The TCR's calculated from these data vary from approximately 1000 ppm/ $^{\circ}\text{C}$  early in the sample life to 4800 ppm/ $^{\circ}\text{C}$  after several firing cycles to 720 $^{\circ}\text{C}$  although the increase was not monotonic. Earlier in the life of both samples, when the resistance could not be accurately measured near room temperature due to instability, slightly lower TCR's were observed.

At several times during the life of the samples measurements were made to detect any time dependence and/or non-linearity in resistance. Time dependence measurements were made with an oscilloscope to detect time constants as small as 1 msec, and with DC current measurements for as long as 20 minutes. No time dependence was observed. The resistance was linear (voltage proportional to current) from 1 $\mu\text{a}$  to 1 ma to within 0.5%. Higher current caused some non-linearity but this is believed to be due to local heating at the point of contact and an increase in resistance due to the TCR of the RuO<sub>2</sub>. Small signal resistance versus DC bias current was also measured with the results that any change in resistance was less than 1%.

There are two reasons why the contact resistance between two massive single crystals would be expected to have characteristics different from that of typical resistors made with small particle size powder. One is that the kinetics of any reactions at the point of contact (e.g., sintering) would be slower by many orders of magnitude; sub-micron diameter crystals would be required to overcome this problem. The second is that the size of the large crystals and their relatively rigid mounting makes it difficult for the interfacial forces of the glass to control the contact forces. In an attempt to overcome this latter problem much smaller, relatively flexible

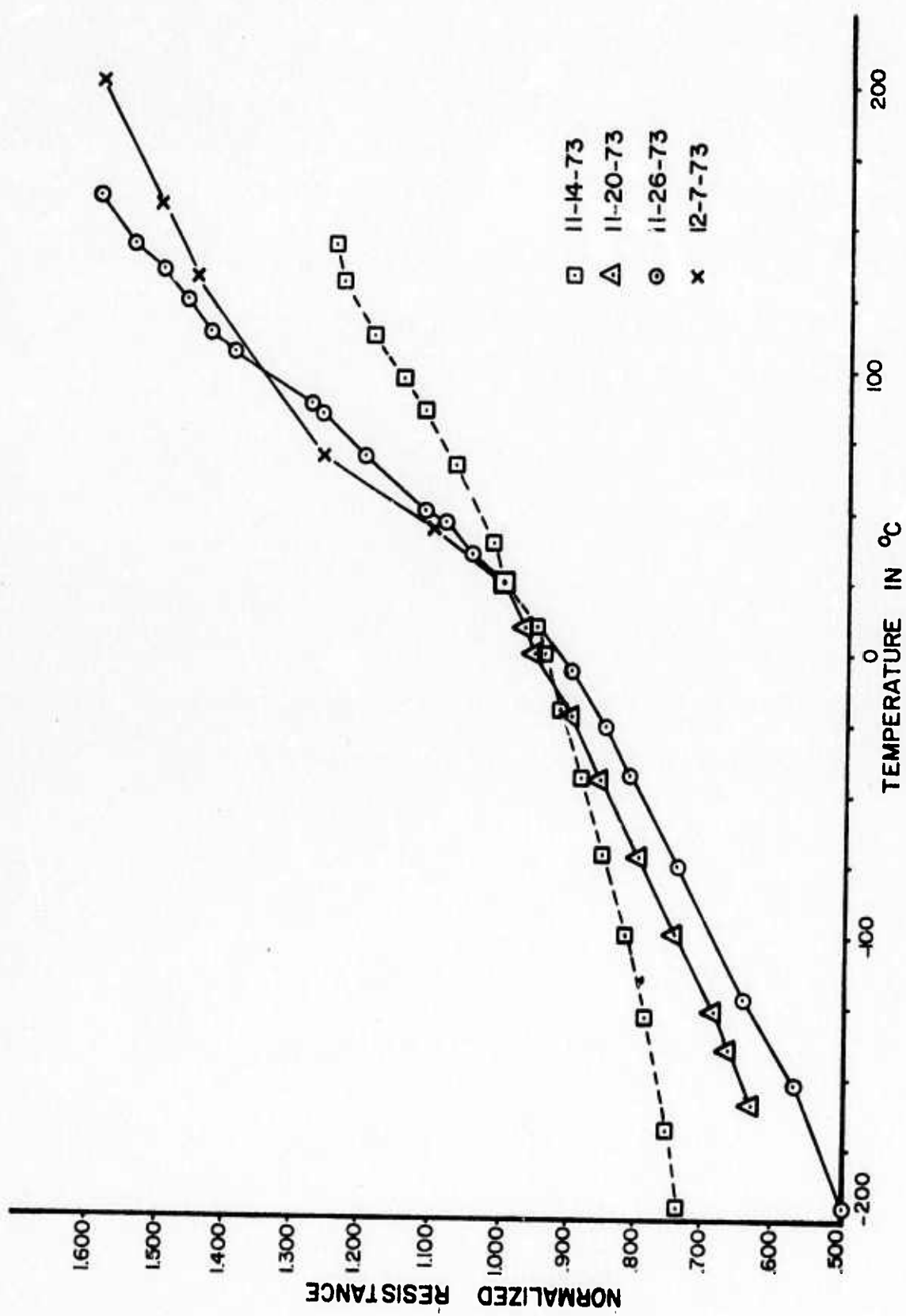


FIGURE 7 -- RESISTANCE VERSUS TEMPERATURE OF CROSSED CRYSTALS

crystals of  $\text{RuO}_2$  have been mounted on 1 mil platinum wires with a single point of contact as shown in Fig. 8 utilizing techniques and materials identical to those reported earlier [17]. The thinner crystal is about  $3\mu\text{m}$  in diameter and 1mm in length, and the other crystal is about  $8\mu\text{m}$  in diameter and 0.8 mm in length. A small quantity of glass encapsulates the region of contact; it was added after both crystals were mounted and in mechanical contact. There are a sufficient number of lead wires to enable four-wire measurement of the contact resistance.

Figure 9 shows the resistance near room temperature ( $86^\circ\text{C}$ ) and the high temperature TCR of the small crossed crystals extrapolated to room temperature as a function of firing time at  $740^\circ\text{C}$ . The resistance was initially just under 3 ohms and increased, mostly after one hour, to 4-5 ohms. During the same time the TCR decreased from approximately  $4000 \text{ ppm}/^\circ\text{C}$  to  $1200 \text{ ppm}/^\circ\text{C}$ . From 100 to 500 hours both the resistance and TCR remained almost constant.

The results with the crossed crystals definitely demonstrated the existence of a conduction mechanism with a TCR lower than that of the contacting materials. In the case of the large crystals that were precoated with glass at the area of contact, attempts to quench the samples at earlier stages of development were unsuccessful at least in terms of useable quantitative data although there was some evidence that the TCR may have been less than  $+1000 \text{ ppm}/^\circ\text{C}$  very early in the life of the conducting contact. Because the glass existed at the point of contact at the beginning of the sample life, and because of the degree to which the glass wets the crystal surfaces, it is considered highly likely that there was glass present at the interface during electrical conduction, but the existence of the glass has not

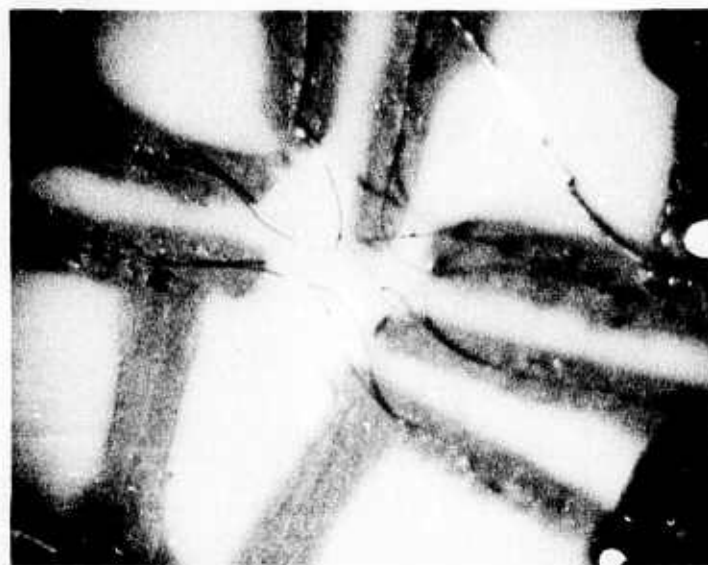


Figure 8a. Mounting Wires on Substrate.

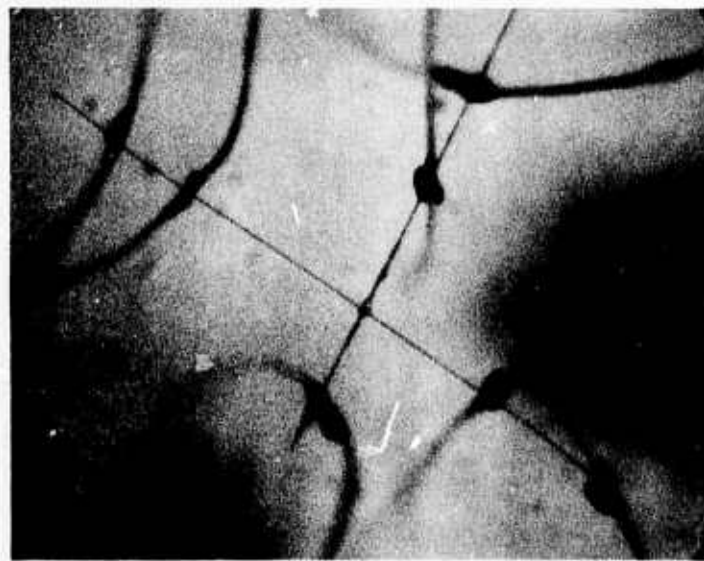


Figure 8b. Mounted Crystals.

Figure 8. Photomicrographs of Small Crossed Single Crystals.

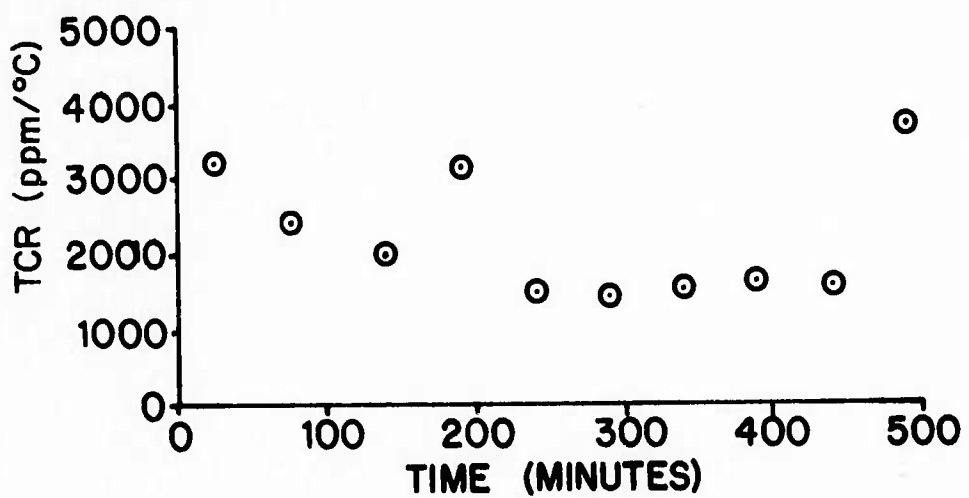
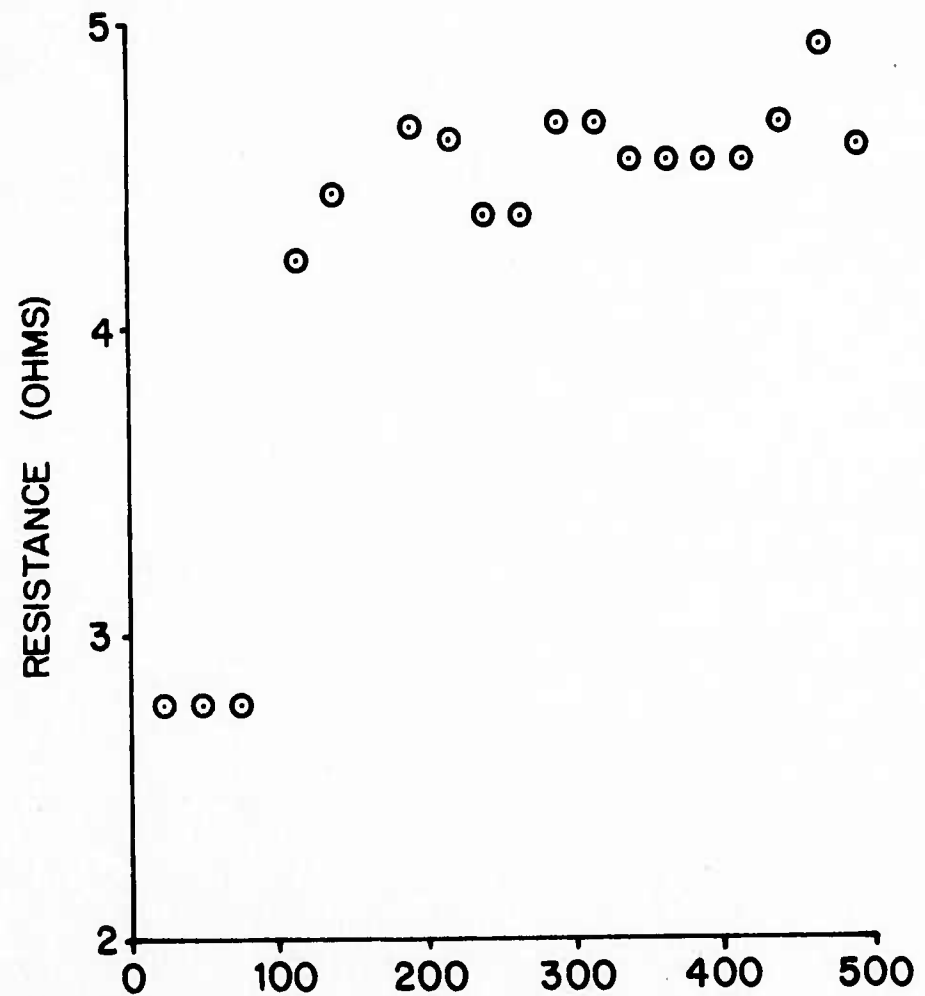


FIGURE 9 -- RESISTANCE AND TCR OF SMALL CROSSED CRYSTALS

been directly confirmed nor has its thickness been determined. For the small crystal sample both crystals were in contact before glass was applied. The contact resistance was erratic before the sample reached the softening point of the glass and the TCR was relatively large at the beginning of the firing process, close to the value of the contacting material. The influence of the glass during firing was both to increase the resistance and decrease the TCR of the contact. The study of contact resistance in a system where particle size prohibits sintering in moderate times is continued below.

#### B. Large Particle Resistors

Preliminary studies of the sintering of RuO<sub>2</sub> in the presence of glass conducted on the video hot stage metallograph have shown that true sintering does not occur between particles in the 100μm size range in reasonable times at 800°C. A neck region between adjacent particles appears to develop but on subsequent treatment with HCl the particles separate; RuO<sub>2</sub> is inert to HCl. In addition, the results of slow firing of resistors discussed in the previous report {18} suggested that two charge transport mechanisms were operative, one involving a well sintered RuO<sub>2</sub> network and the other associated with poorly sintered contacts. In order to further develop these concepts a series of experiments were conducted under conditions where only the poorly sintered contacts should develop.

Two resistor-like samples were prepared using particles of RuO<sub>2</sub> in the size range of 150 to 180 μm. The average particle size of RuO<sub>2</sub> in a typical resistor is less than 1 μm. The particles were mixed with the lead-borosilicate glass powder and a small amount of screening agent; this formulation was applied with a pick in a thin, nearly uniform layer to a substrate with four conductive

terminals. Screen printing was not feasible because of the particle size. Figure 10 shows the first sample, sample 85, after several high temperature firings.

Firing to  $650^{\circ}\text{C}$  for  $2\frac{1}{2}$  hours failed to result in electrical continuity. At this stage the sample had a very large concentration of bubbles and small fractures throughout the resistor structure. Firing to  $730^{\circ}\text{C}$  for 15 minutes removed most of the bubbles and allowed the glass to flow away from the  $\text{RuO}_2$  area resulting in a more compact film, and the resistance decreased to about 20 ohms at room temperature. Fractures of the glass were still prevalent in the cooled sample, as can be seen in Fig. 10b. These fractures always existed at room temperature throughout the life of both samples and, because of the small number of contacts in the conducting paths, influenced resistance value. During temperature changes of the resistor, step changes in resistance value were frequently noted; these are assumed to be due to the occurrence of one or more fractures. Figure 11 shows resistance versus temperature for sample 85; it has a TCR of  $3750 \text{ ppm}/^{\circ}\text{C}$  at room temperature. Figure 12 shows resistance versus temperature for the second sample, sample 88, that was measured during heating to  $510^{\circ}\text{C}$  and subsequent cooling to room temperature. From room temperature to  $200^{\circ}\text{C}$  (the same as the range for Fig. 9), the TCR is  $+3700 \text{ ppm}/^{\circ}\text{C}$  in agreement with the results obtained with sample 85. Above this temperature the TCR is negative, however, at approximately the softening temperatures of the glass ( $450^{\circ}\text{C}$ ), the resistance increased by several orders of magnitude going beyond the range of the resistance measuring circuit being used. This general type of behavior is consistent with observed properties of resistors and earlier crossed crystal measurements. On cooling,



Figure 10a. Resistor Geometry.

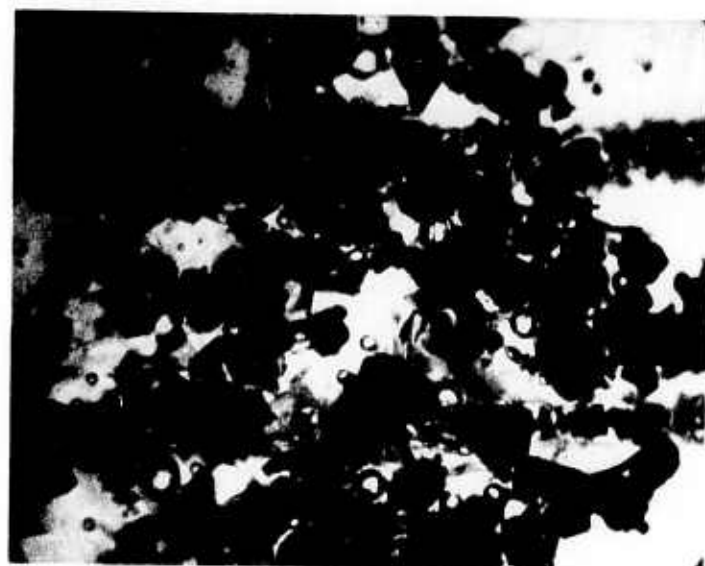


Figure 10b. Detailed View Showing Fractures.

Figure 10. Large Particle Resistors.

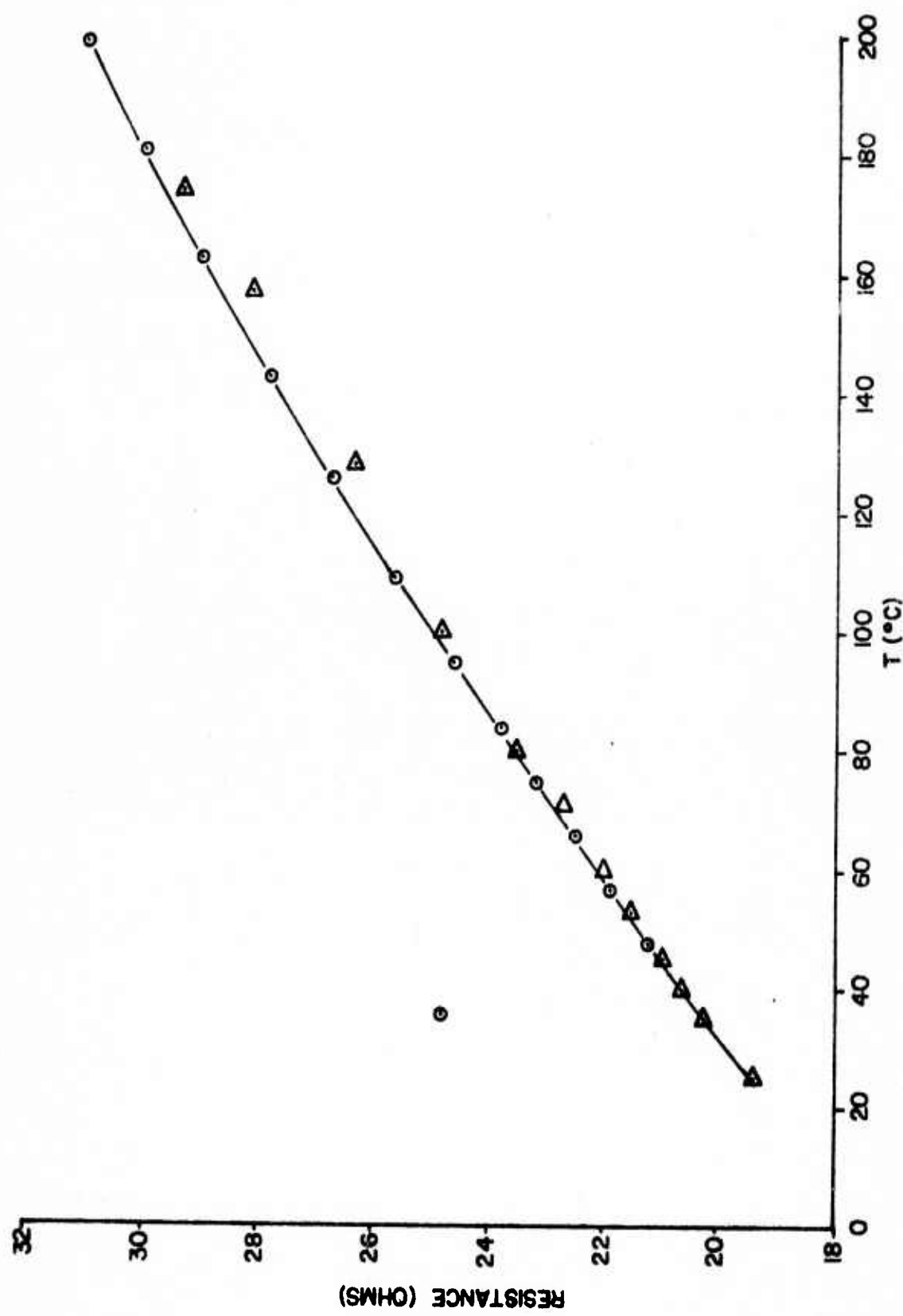


FIGURE 11. — RESISTANCE VERSUS TEMPERATURE OF LARGE PARTICLE RESISTORS

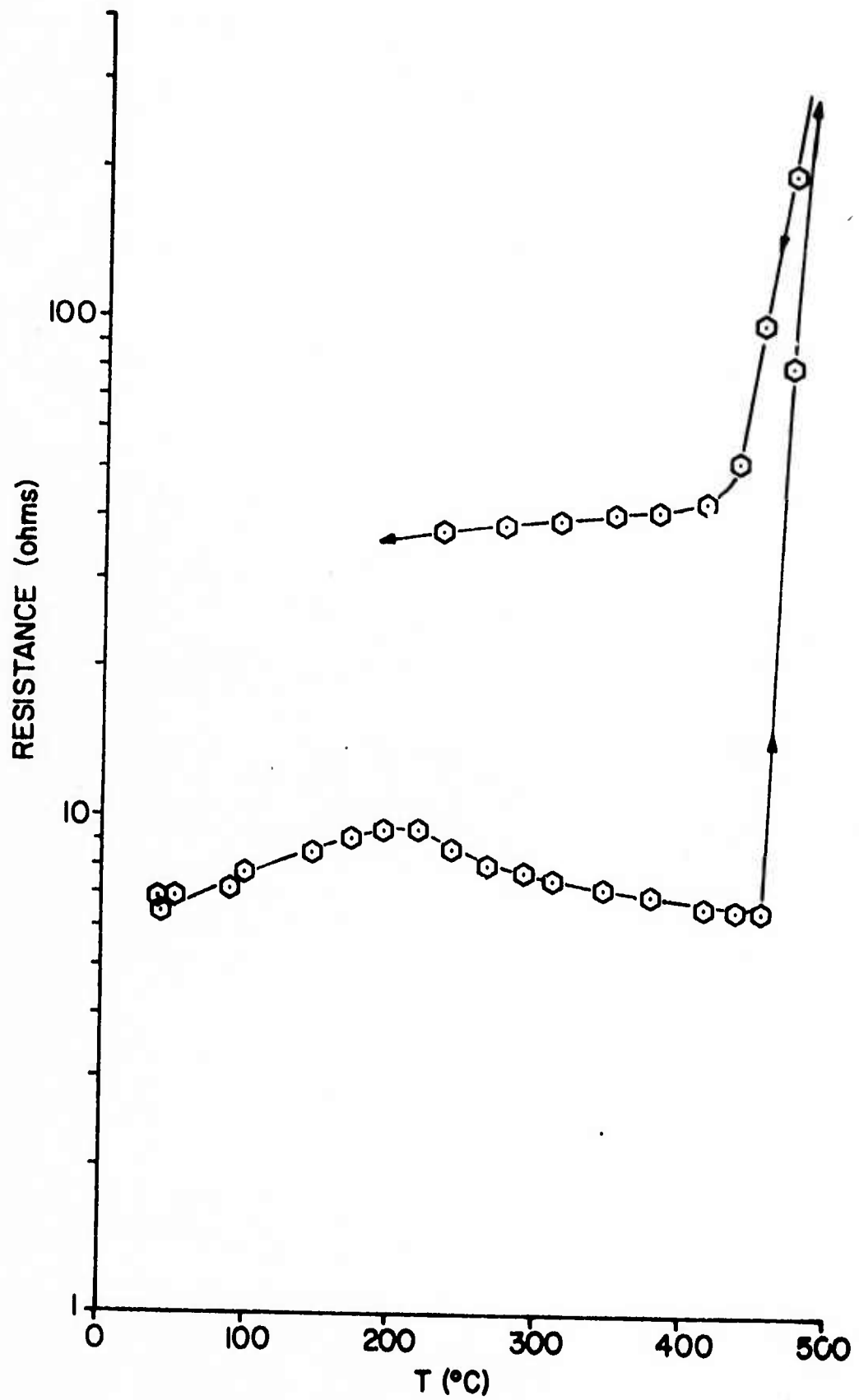


FIGURE 12 -- RESISTANCE VERSUS TEMPERATURE DURING FIRING OF LARGE PARTICLE RESISTORS

the sample was approximately ten times higher in resistance value than on heating but had a TCR with respect to room temperature of only 1460 ppm/ $^{\circ}$ C. There was a step change in resistance value at 210 $^{\circ}$ C that terminated the usefulness of the sample.

In terms of the number of conducting contacts, the large particle resistors are between the single contact crossed crystal samples and more typical resistors. In terms of microstructure development that depends on particle size, however, the samples should be most similar to the crossed crystal samples. The range of TCR's obtained with these large particle resistors is consistent with this prediction. Even the problems of glass fracture are similar. As with the crossed crystals, a conduction mechanism was created that seems to be different from that predicted from the properties of single crystal RuO<sub>2</sub>, and is believed to be similar to one of the mechanisms operative in actual resistors.

### C. Low Temperature Resistance Measurements

Resistance versus temperature measurements for thick film resistors containing 10% RuO<sub>2</sub> were extended to lower temperatures by utilizing the sample fixture shown in the cutaway diagram of Fig. 13. The main body of the fixture is copper to provide for temperature stability and ease of measurement. Four spring-loaded probes, insulated by Teflon, make contact to the conductive pads on the substrate; wires from the probes lead to the measurement system. A thermocouple (iron-constantan) is embedded directly under the sample to monitor substrate temperature. A heater winding of #36 gauge Cupron wire is used for increasing the rate of temperature rise of the sample. In normal use, the fixture is lowered into a dewar which is then filled with liquid nitrogen to completely cover the sample fixture.

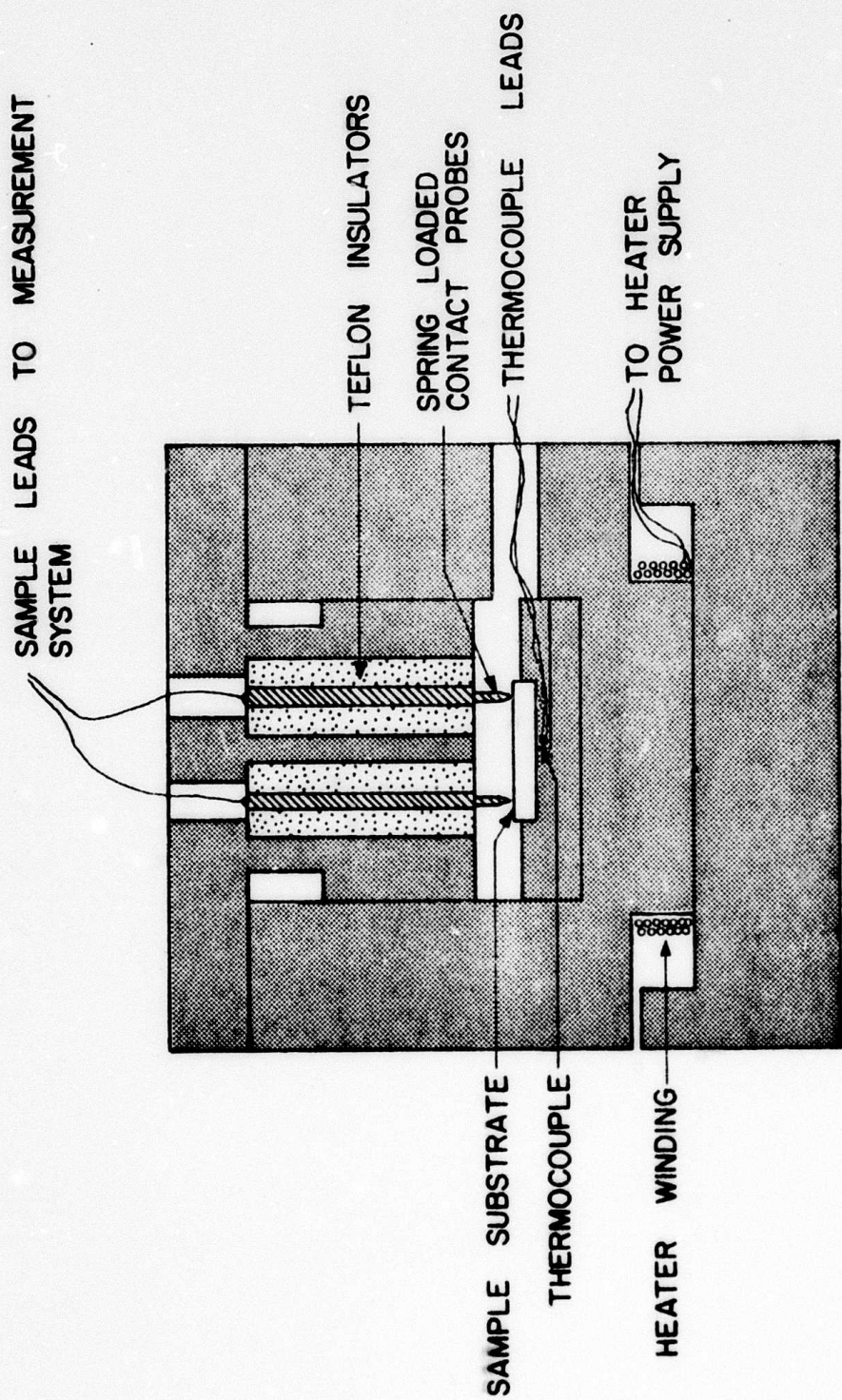


FIGURE 13 -- LOW TEMPERATURE RESISTANCE AND TEMPERATURE MEASURING FIXTURE

After the data point at  $-196^{\circ}\text{C}$  is taken, the fixture is removed from the dewar and allowed to warm slowly in a room temperature environment while the resistance is continually recorded. The rate of temperature increase is consistent with the ease of measurement in reasonable time except above  $-50^{\circ}\text{C}$  where the heater is used.

Figure 14 shows the normalized resistance versus temperature of three  $10\%$   $\text{RuO}_2$  resistor samples fired for varying times at  $630^{\circ}\text{C}$ . Sample 78 was fired for 20 minutes and has the most negative TCR at room temperature sample 74 was fired for 40 minutes and has an intermediate TCR; sample 77 was fired for 90 minutes with a resultant positive TCR at room temperature. The data points at  $-296^{\circ}\text{C}$  (approximately  $4^{\circ}\text{K}$ ) were taken with the sample immersed in liquid helium using a different sample measuring system.

The more "rare" samples exhibit a modest negative TCR at room temperature and strong negative dependence at low temperatures which can be described by an exponential relationship. This is the type of temperature dependence expected for poorly sintered contacts between conductive oxide particles in a glassy matrix. On the other hand, the "well done" samples show a slightly positive or near zero TCR over most of the temperature range indicative of a better sintered conductive network.

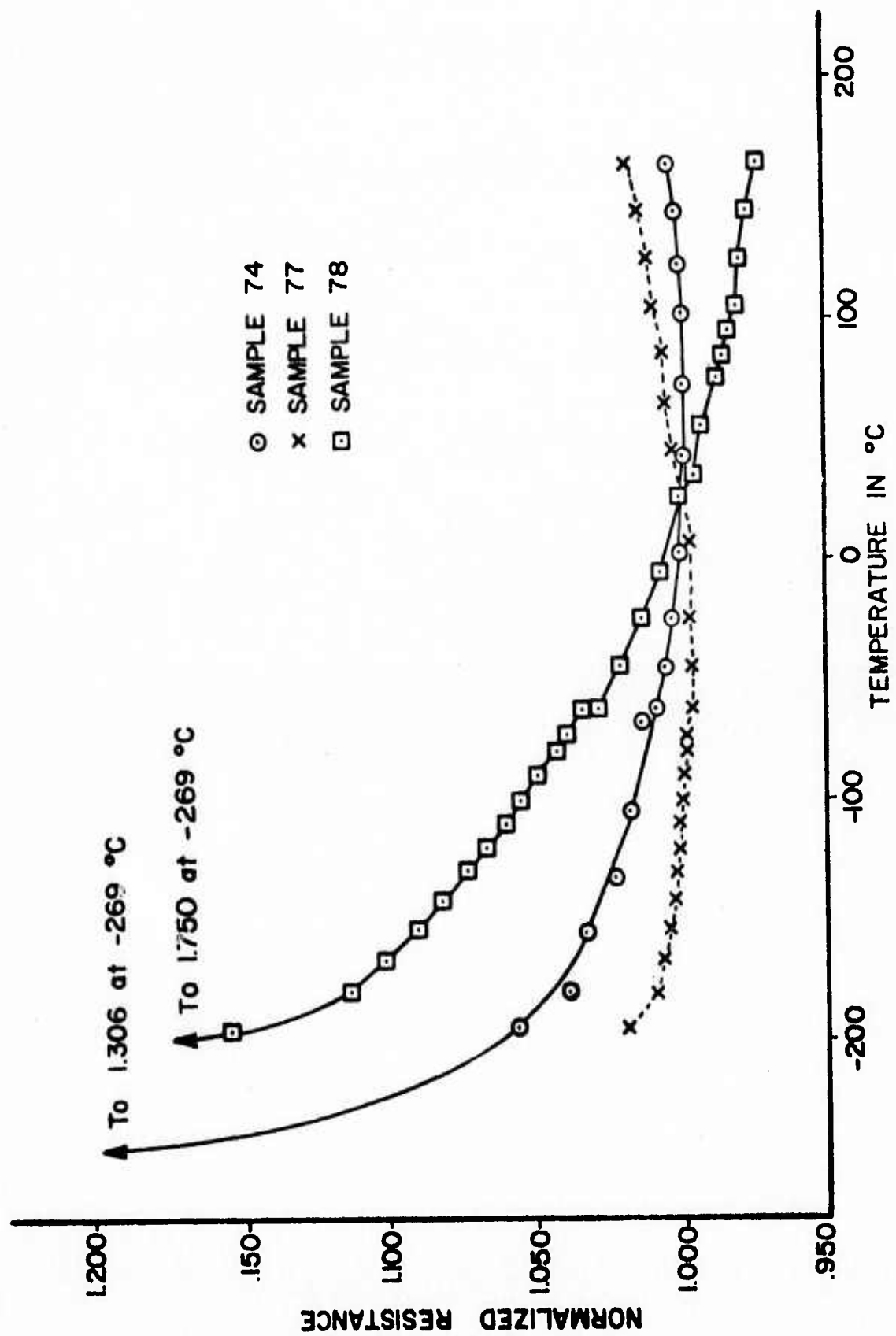


FIGURE 14 -- NORMALIZED RESISTANCE OF RESISTORS VERSUS LOW TEMPERATURE

#### IV. Industrial Coupling

##### A. Search for a new screening agent

Screening agents normally consist of a solution of a polymer in a suitable solvent and several other modifiers in intermediate levels of concentration to improve bleedout, leveling, etc. These modifiers have not been used in this study because they increase the chemical complexity of the screening agent. The solvent ideally has a low vapor pressure at room temperature but evaporates readily at higher temperatures. The combination of solid polymer and solvent has two practical advantages:

- (1) A pseudoplastic rheology that results in screenable materials can readily be obtained; and (2) it is possible to remove the solvent during drying leaving the solid polymer, thereby creating a mechanically durable film prior to higher temperature processing. The combination used in this project and discussed earlier<sup>(19)</sup> is ethyl cellulose dissolved in Butyl Carbitol. The viscosity and drying characteristics have been adequate for the performance requirements of this study and the chemical system is simple, as desired. However, careful observation during weight loss measurements of pure polymer, no addition of solvent or inorganics, have shown that the high temperature removal of the ethyl cellulose polymer results in a potentially reducing atmosphere in the film. Although the quantity is too small for the resolution of our measuring system, a dark brown residue exists between 350 and 750°C. There is also a dark brown discoloration in thicker than normal glass films (otherwise colored white); this discoloration is not present above 800°C. In films containing RuO<sub>2</sub> this carbonaceous residue could easily reduce the oxide to the metal. Since the kinetics of reoxidation are very slow, this would be a permanent

change in the critical ingredient of the resistor. No discoloration of screened films has been noticed when firing in air atmosphere but some small amount of residue is presumed to exist.

In order to find a more suitable polymer an extensive literature survey was conducted to find polymers whose thermal decomposition in the presence of oxygen was known to be as free as possible of reducing effects and to be as low in temperature as possible (<300°C is desirable in order to be absent during initial stages of sintering of the smaller glass particles). Unfortunately, virtually no information was found on the decomposition of the more promising polymers in an oxidizing atmosphere; all data are for thermal decomposition in vacuum because of several practical considerations of chemical analysis.

Based on the data obtained with vacuum decomposition the two most promising polymers were polyalphamethylstyrene and polymethymethacrylate (MMA). Less desirable because of decomposition temperatures were polyoxymethylene and polyethylene oxide; polyoxymethylene has the additional disadvantage of decomposing into formaldahyde. The better two polymers are consistent with the recommendations of L. F. Miller {20} who reported their use in thick films but did not report any quantitative data on decomposition rates. Both materials have been selected for further study but only the evaluation of polyalphamethylstyrene is reported; the evaluation of MMA is still in progress.

#### B. Evaluation of Polyalphamethylstyrene

The polyalphamethylstyrene used for this study were Dow types 276-V2 and 276-V9. Both are viscous liquids at room temperature; V-2 has a viscosity of 22 Kcps at shear rates from 5 to 40 sec<sup>-1</sup>. The fact that the polymers are liquids is due to their limited molecular weight. The

tendency to decompose is great at the elevated temperatures where polymerization takes place. The polymerization reactions occur at temperatures at which the depolymerization rate prohibits molecular weights large enough to result in solid plastic. The viscosity is high enough to be usable for screening agents. Figure 18 shows the evaporation of poly-alphamethylstyrene at the constant temperatures of  $293^{\circ}\text{C}$  and  $400^{\circ}\text{C}$ . The results were obtained with 80 to 90 milligram samples heated in crucibles 6 mm in diameter in the TGA system described earlier<sup>{21}</sup>. It can be seen that the ideal goal of complete removal at  $300^{\circ}\text{C}$  is not possible with this material, at least in reasonable time. At  $400^{\circ}\text{C}$  complete removal is obtained in about 45 minutes. The evaporation at a constant heating rate of  $9.5^{\circ}\text{C}/\text{minute}$  is compared to that of ethyl cellulose in Fig. 16 . The two styrenes evaporate more rapidly at the beginning, near  $250^{\circ}\text{C}$ , but more importantly, the last traces of resin leave rapidly. These measurements indicate that either styrene resin would be superior to that ethyl cellulose.

Visual observations also indicate that polymer removal is more complete in the case of the styrenes; there is no residue in the weight loss crucibles at the termination of an experimental run. No discoloration is observed in screen printed films either, although this is also the case with ethyl cellulose. Figure 17 shows that this discoloration was present in sufficiently thick films along with demonstrating other effects on firing characteristics. Two samples were made from complete formulations (polymer + solvent + glass), and one from a formulation containing polymer and glass only. The films, initially about 1mm thick in the bottom of shallow alumina crucibles, were dried at  $400^{\circ}\text{C}$  for one hour then fired to  $650^{\circ}\text{C}$  for 10 minutes. It can be seen that in addition to color, the residue has

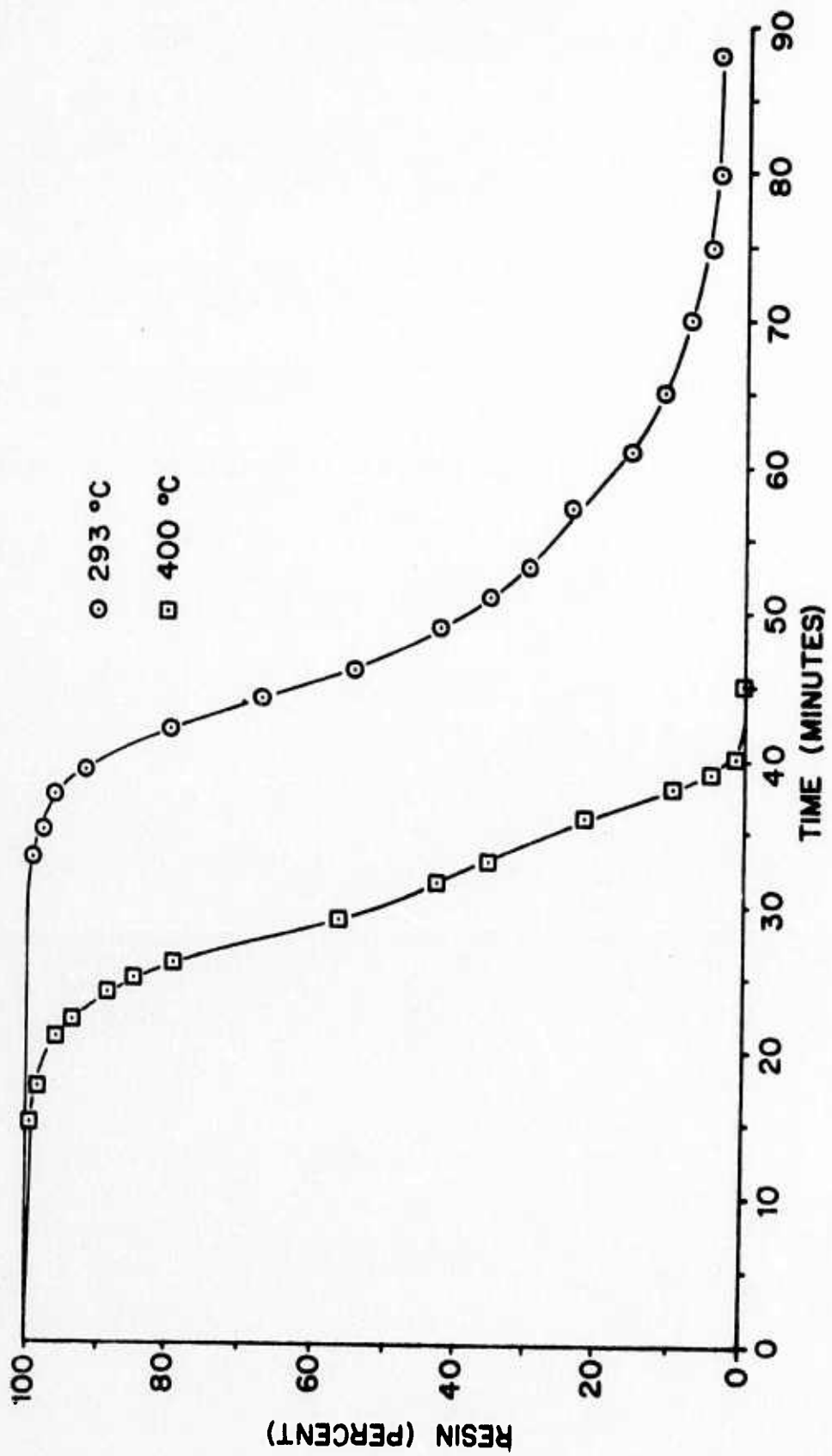


FIGURE 1E -- EVAPORATION OF POLYALPHAMETHYLSTYRENE AT CONSTANT TEMPERATURES

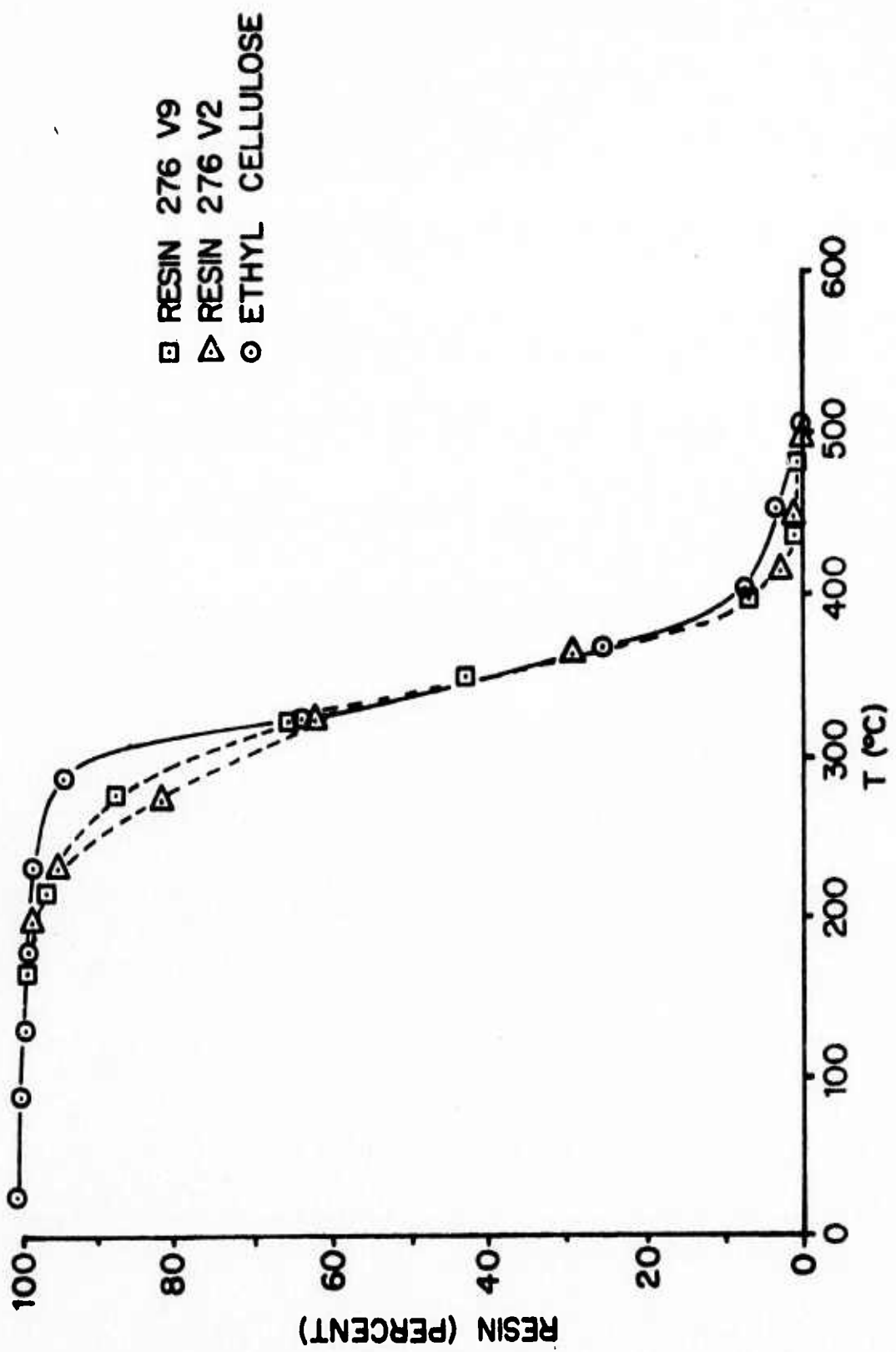


FIGURE 16 -- COMPARISON OF EVAPORATION RATES



a. ethyl cellulose  
butyl carbitol  
glass

b. 276-V2  
styrene  
butyl carbitol  
glass

c. 276-V2  
styrene  
glass

Figure 17 Results of Firing Glass Formulations

affected interfacial energies (wetting) significantly and differently. The ethyl cellulose residue has caused "blistering", a not uncommon problem with some commercial inks.

Viscosity and other screening parameters of polyalphamethylstyrene formulations are similar to the ethyl cellulose formulation. The mixture of glass and polymer alone is too viscous and is sticky and stringy. However, small additions of Butyl carbitol cure these problems. Fig. 18 shows the viscosity of 40 v/o glass formulations using both types of screening agents; they are as close as can be expected. Bleedout and printed film thickness are also similar.

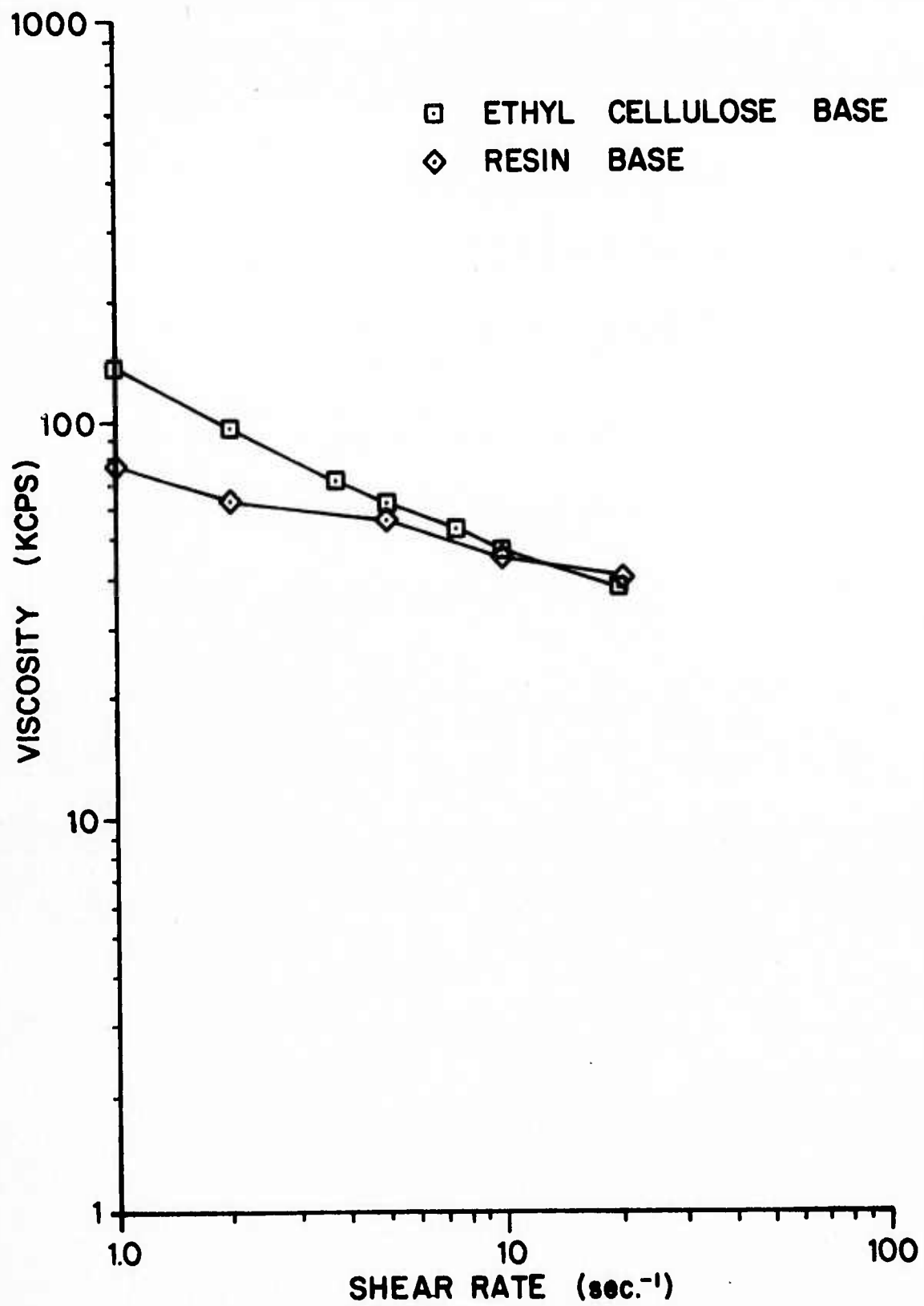


FIGURE 18 -- COMPARISON OF VISCOSITY VERSUS SHEAR RATE

## V. Summary and Future Plans

### A. Microstructure Development

Quantitative results from the glass sintering studies have proven that viscous flow is the dominant mechanism operative, and are therefore consistent with the sequential sintering model proposed previously. The viscosity and surface tension results at elevated temperatures will be utilized in developing the quantitative sintering model.

Measurements of the sintering kinetics of RuO<sub>2</sub> in the presence of glass will be continued. The techniques previously developed to arrest the microstructure development at various stages will be utilized in conjunction with SEM studies of the microstructure to obtain the remaining parameters required for a phenomenological model.

### B. Charge Transport Mechanisms

Studies of the electrical properties of a single contact between RuO<sub>2</sub> single crystals have shown a charge transport mechanism that leads to a TCR lower than that of bulk RuO<sub>2</sub> and one that varies with time at firing temperature. This behavior was confirmed with studies of large particle size resistors in which sintering of RuO<sub>2</sub> does not occur during the time-temperature relationships employed. These studies clearly demonstrate that charge transport can occur in the RuO<sub>2</sub>-glass composite system by mechanisms other than one involving a continuous polycrystalline RuO<sub>2</sub> network. Similar studies will continue during the coming period in order to obtain a quantitative description of this charge transport mechanism.

### C. Test of Models

The sheet resistance and TCR of resistors and conductors will be determined as a function of volume fraction of conductive phase to glass, and as a function of particle size of the conducting phase and of the glass. The important glass parameters, viscosity and surface tension, will be varied at constant thermal expansion and the results compared with predictions of the microstructure model and the interface model. Chemical additives which will alter the electrical properties according to the interface model but which will not affect microstructure development will be utilized to further test the interface model. Predictions of the microstructure and the interface model will be utilized to develop optimum resistor and conductor formulations within the given materials system. The performance of these will be evaluated according to the list of specifications developed previously.

## REFERENCES

1. R. W. Vest, Semi-annual Technical Report for the period 7/1/70-12/31/70, Purdue Research Foundation Grant No. DAHC-15-70-G7, ARPA Order No. 1642, Feb. 1, 1971.
2. R. W. Vest, Semi-Annual Technical Report for the period 7/1/71-6/30/71, Purdue Research Foundation Grant No. DAHC-15-70-G7, ARPA Order No. 1642, August 1, 1971.
3. R. W. Vest, Semi-annual Technical Report for the period 7/1/71-12/31/71, Purdue Research Foundation Grant No. DAHC-15-70-G7, ARPA Order No. 1642, Feb. 1, 1972.
4. R. W. Vest, Semi-annual Technical Report for the period 1/1/72-6/30/72, Purdue Research Foundation Grant No. DAHC-15-70-G7, ARPA Order No. 1642, August 1, 1972.
5. R. W. Vest, SEMi-annual Technical Report for the period 7/1/72-12/31/72, Purdue Research Foundation Grant No. DAHC-15-70-G7, ARPA Order No. 1642, Feb. 1, 1973.
6. R. W. Vest, Semi-annual Technical Report for the period 1/1/73-6/30/73, Purdue Research Foundation Grant NO. DAHC-15-70-G7, ARPA Order No. 1642, August 1, 1973.
7. Page 3, Reference 3
8. Page 8, Reference 5
9. Leo Shartsis, et al., "Viscosity and Density of Molten Optical Glasses," J. Res. NBS, 46, 176 (1951).
10. Leo Shartsis, et al., "Surface Tensions of Some Optical Glasses," J. Am. Cer. Sec., 30, 130 (1947).
11. Page 31, Reference 1

12. Leo Shartsis, et al., "Surface Tension of Compositions in the Systems PbO-B<sub>2</sub>O<sub>3</sub> and PbO-SiO<sub>2</sub>," J. Am. Cer. Soc., 31, 23 (1948).
13. Page 8, Reference 5
14. G. L. Fuller, "Microstructure and Mechanisms of Electrical Conduction in Ruthenium Dioxide-Glass Thick Film Resistors," Ph.D. Thesis, Purdue University, June 1971, page 175.
15. Page 16, Reference 2
16. Page 15, Reference 5 and Page 20, Reference 6
17. Page 22, Reference 1
18. Page 25, Reference 6
19. Page 20 and 42, Reference 6, Page 30, Reference 5, Page 27, Reference 4
20. L. F. Miller, "Glaze Resistor Paste Preparation," Proc. IEEE Comp. Conf., 1970, p. 92-101.
21. Page 31, Reference 5